

Supporting Information

Highly Selective Sensing of C₂H₆O, HCHO, and C₃H₆O Gases by Controlling SnO₂ Nanoparticle Vacancies

Lingyue Liu, Shaoming Shu, Guozhu Zhang and Shantang Liu *

Key Laboratory for Green Chemical Process of Ministry of Education and School of Chemistry
and Environmental Engineering, Wuhan Institute of Technology, Xiongchu Avenue, Wuhan
430073, China

*Corresponding author. E-mail: stliu@wit.edu.cn (S. Liu); fax: (+86) 027-87195001

Experimental Section

Chemicals. Tin chloride (SnCl_4), Urea, Sodium DL-lactate, Ethylene glycol, Glycerol, Ethanol, Formaldehyde solution, Methanol were purchased from Sinopharm Chemical Reagent Co., Ltd. (Shanghai, China). Acetone, Toluene were purchased from Tianjin TIANLI Chemical Reagents Ltd. (China). All the reagents were analytical grade and used directly without further purification.

Preparation. In a typical synthesis, 40 g of ice and 3.91 g (15 mmol) of Tin chloride (SnCl_4) were heat until dissolved, then 5 g urea were added into the solution under vigorous stirring. Afterwards, the mixture was added to the sodium lactate 5 ml. The obtained transparent solution was transferred to a Teflon-lined stainless steel autoclave to perform solvothermal process at 200 °C for 20 h. After cooling down to room temperature naturally, the solid product was collected by centrifugation and washed with deionized water and ethanol for three times. The sample was finally dried in a vacuum oven for 12 h at 80 °C. By calcining the sample at 500 °C for 4h in different atompheres (Air, He, O_2). The obtained sample **S-A** (air), **S-H** (helium), **S-O** (oxygen) for further characterization.

Characterization. X-ray powder diffraction (XRD) was carried out on Bruker axs D8 Discover (Cu K = 1.5406 Å) at a scan rate of 2° min^{-1} in the 2θ range from 10 to 80° . Transmission electron microscopy (TEM) were recorded on a Philips Tecnai G2 20 electron microscope, using an accelerating voltage of 200 kV. Samples for TEM analysis were prepared by drying a drop of nanocrystal dispersion in absolute ethanol on carboncoated copper grids. The electron spin resonance (ESR) spectra of obtained samples were carried out a Bruker EMX 10/2.7 ESR spectrometer (Billerica, MA). Photoluminescence (PL) of the samples spectra were recorded on a Hitachi F4600 spectroscopy. Brunauer-Emmett-Teller (BET) specific surface area of the powders was analyzed by nitrogen adsorption in a Micromeritics ASAP 2020 nitrogen adsorption apparatus (USA). All the as-prepared samples were degassed at 150 °C for 4 h prior to nitrogen adsorption measurements.

Positron Annihilation Measurement. The positron lifetime spectrum were measured using a conventional fast-fast coincidence system with a time resolution of about 220 ps in full width at

half-maximum. A 20MCi positron source of ^{22}Na was sandwiched between two identical pieces of samples, and the total count was about 10^6 counts were accumulated for each spectra. Positron lifetime calculations were performed using the atomic superposition (ATSUP) method.¹⁻² The electron density and the positron crystalline Coulomb potential are constructed by the non-self-consistent superposition of free atom electron density and Coulomb potential in the absence of the positron. The electron-positron enhancement factor was used in the positron lifetime calculations, which was described within the generalized gradients approximation by Barbiellini.³ Positron lifetime calculations were performed for unrelaxed structure monovacancy defects and vacancy associates in SnO_2 using $3 \times 3 \times 2$ supercells.

In situ Diffuse Reflectance Infrared Fourier Transform Spectroscopy (DRIFTS) Measurement.

DRIFT spectra were recorded on a Bruker Tensor 27 FTIR Spectrometer equipped with a KBr beam splitter and a mercury-cadmium-telluride (MCT) detector cooled by liquid N_2 . DRIFT spectra were operating between 800 and 4000 cm^{-1} using a Harrick reaction chamber with KBr windows and a Harrick DRA-2C1 diffuse reflectance accessory. The vacuum chamber was connected to gas lines for treating samples, and its temperature was controlled by a programmer from room temperature to $600\text{ }^\circ\text{C}$. Spectra were recorded at a resolution of 4 cm^{-1} , and 64 scans were averaged for background spectrum and sample spectrum in a time resolution of 1 min. In the DRIFTS experiment, a 100 mg sample (annealed at $500\text{ }^\circ\text{C}$ for 3 h) was located in the sample holder of the vacuum cell by using a filling device to obtain reproducible reflecting planes. The sample layer was 3 mm thick. Spectra were measured in absorbance. During target gas (ethanol, formaldehyde and acetone) exposure, the in situ DRIFTS analyses were continuously performed. Prior to each test, all samples were held at $300\text{ }^\circ\text{C}$ under vacuum for 30 min to remove the adsorbed water on the sample. After cooled to the desired temperature to get a background spectrum, and this spectrum was then subtracted from the sample spectra for each measurement. The 500 ppm ethanol, formaldehyde and acetone in air was flowed into the cell at 40 mL min^{-1} controlled by mass flow control meter and the spectra were recorded at the reaction time 0.5, 1, 2, 3, 5, 10, 20 min.

Sensor fabrication and gas sensing measurement. The as-synthesized products were ground and mixed with ethylene glycol, glycerol and H_2O (2:2:1, mass ratio) to form a paste, and then the

paste was dropped onto an Al_2O_3 ceramic plate substrate ($8 \text{ mm} \times 10 \text{ mm} \times 0.65 \text{ mm}$) to form a thick film between a pair of Au interdigitated electrodes (electrode width 0.2 mm, gap width 0.2 mm) that had been previously printed on the substrate, followed by drying at $120 \text{ }^\circ\text{C}$ for approximately 6 h and a subsequent annealing at $300 \text{ }^\circ\text{C}$ for another 2 h under synthetic air flow.

The gas-sensing properties of the sensors were measured using a CGS-1TP intelligent test system (Beijing Elite Tech. Co., Ltd., China). The measurement was processed by a static process in a test chamber (18 L in volume) with environmental air relative humidity about 25% and room temperature about $25 \text{ }^\circ\text{C}$. This sensing setup is similar to those used previously by our research group. Firstly, the sensors were placed into the chamber and preheated at their work temperature. Then, a given amount of the tested gas was injected into the test chamber. When the response reached a constant value, the upper cover of the test chamber was removed and the sensor began to recover in air. The response of the sensor was defined as $(S = R_a/R_g)$, where R_a and R_g represent the resistances of the sensor in the air and the target gas, respectively. The response and recovery times were defined as the time taken by the sensor to achieve 90% of the total resistance change in the cases of adsorption and desorption.

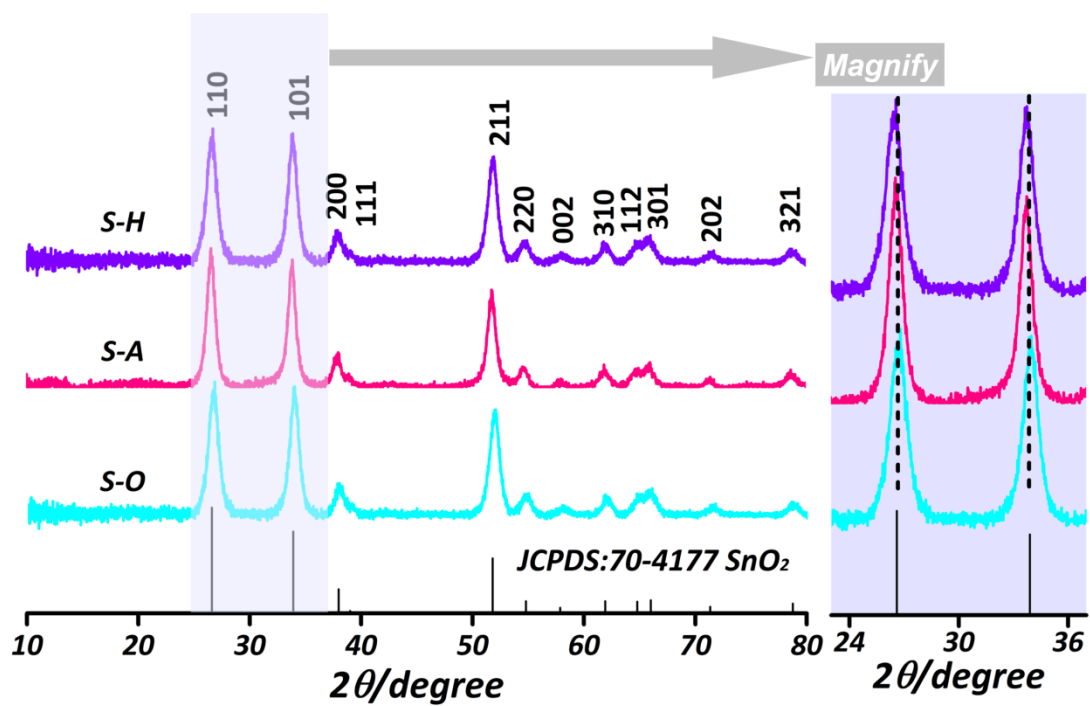


Figure S1. XRD patterns of SnO₂ nanoparticle fabricated from air (S-A), He (S-H), and O₂ (S-O), respectively.

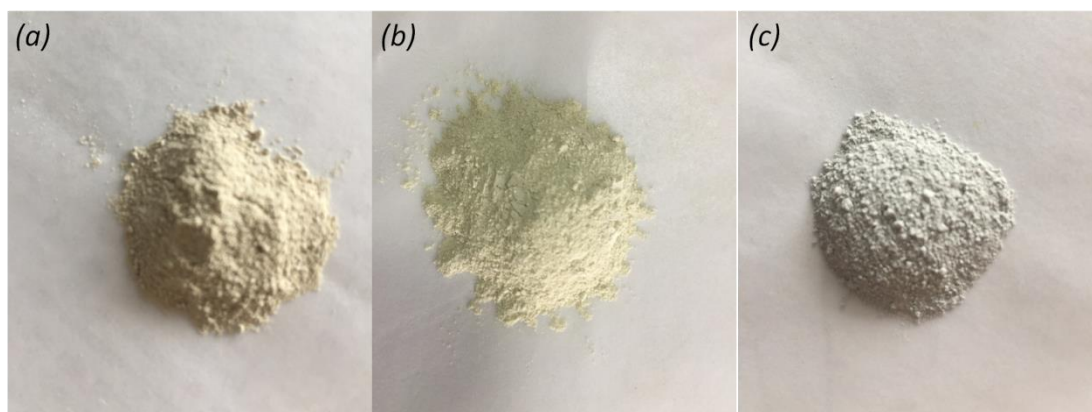


Figure S2. (a), (b) and (c) are photographs of samples of SnO₂ nanoparticles calcined in air (S-A), He (S-H) and O₂ (S-O), respectively.

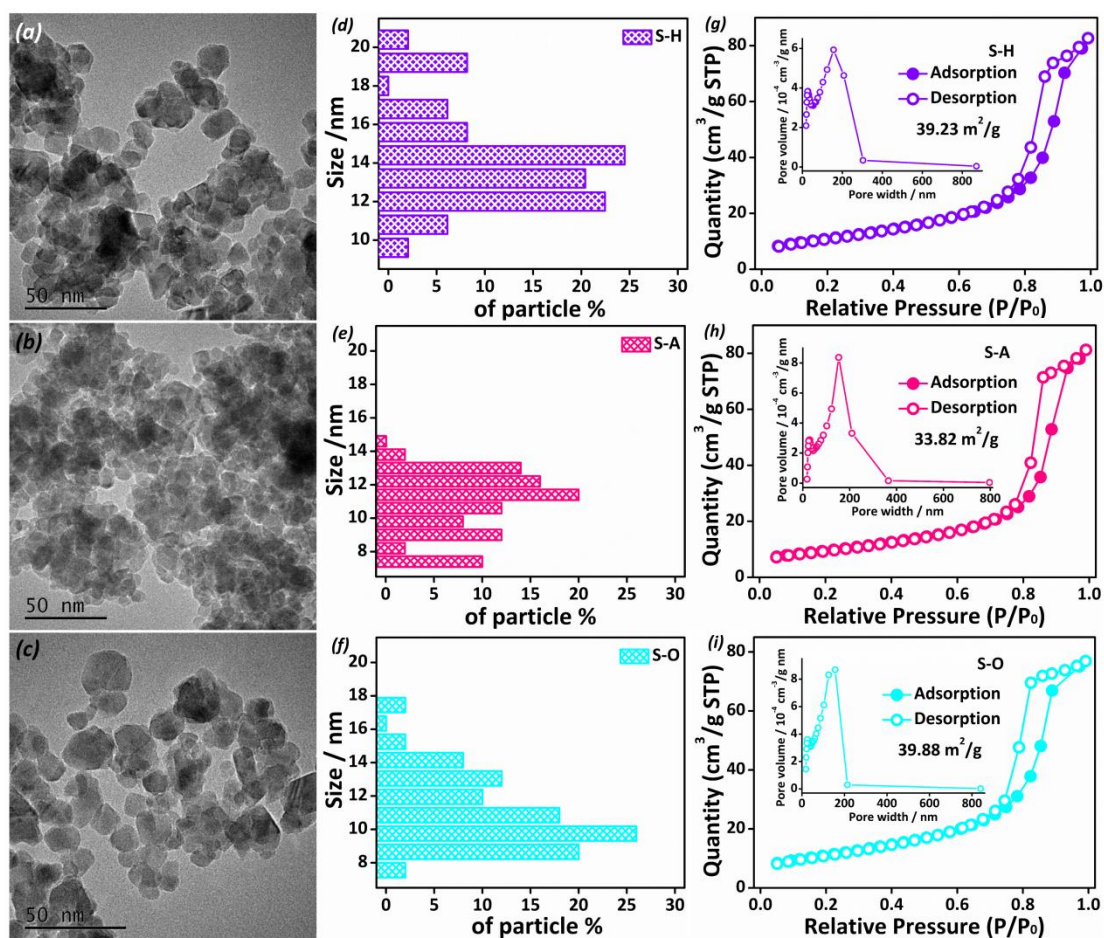


Figure S3. TEM images and corresponding size histograms for (a, d) S-A, (b, e) S-H, and (c, f) S-O. (g, h, i) N₂ adsorption/desorption isotherm of the as-prepared S-A, S-H and S-O. The inset shows the pore size distributions calculated using the BJH method.

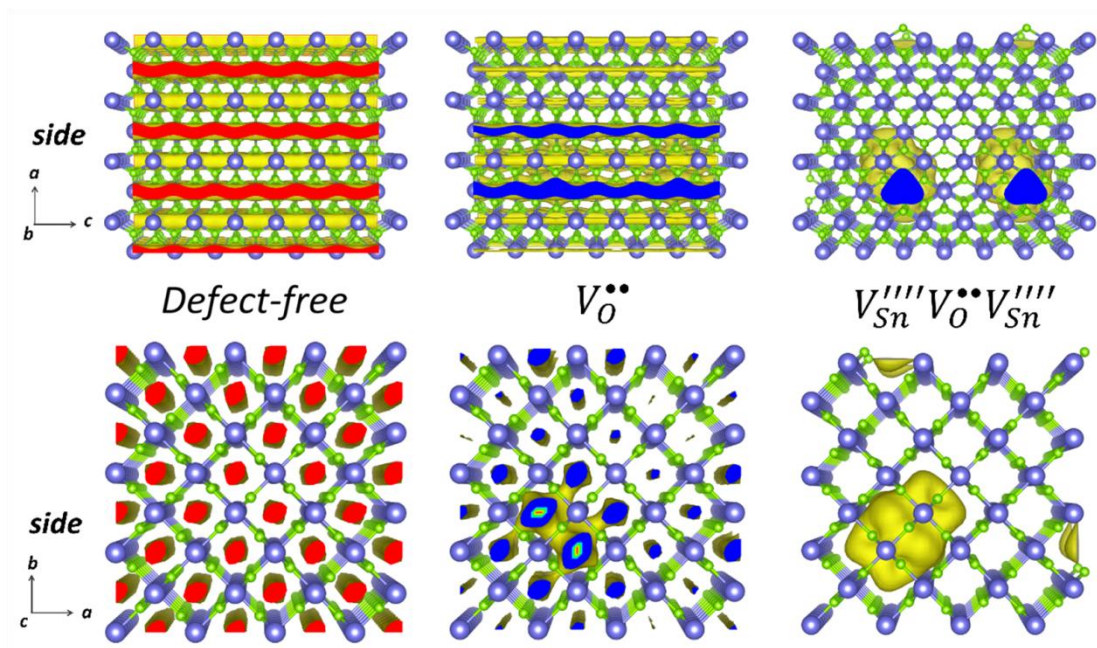


Figure S4. Positron density distribution in SnO₂ with different types of defect cluster, respectively.

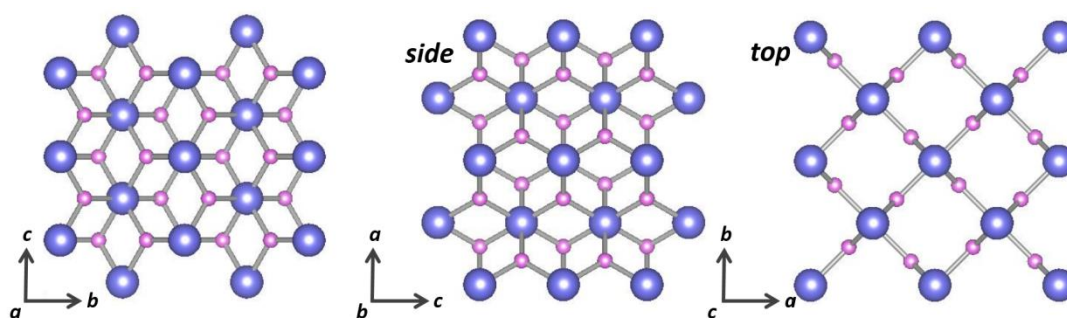


Figure S5. Schematic representation of the crystal structure of SnO₂. Three-dimensional projection and along with the side and top view, respectively.

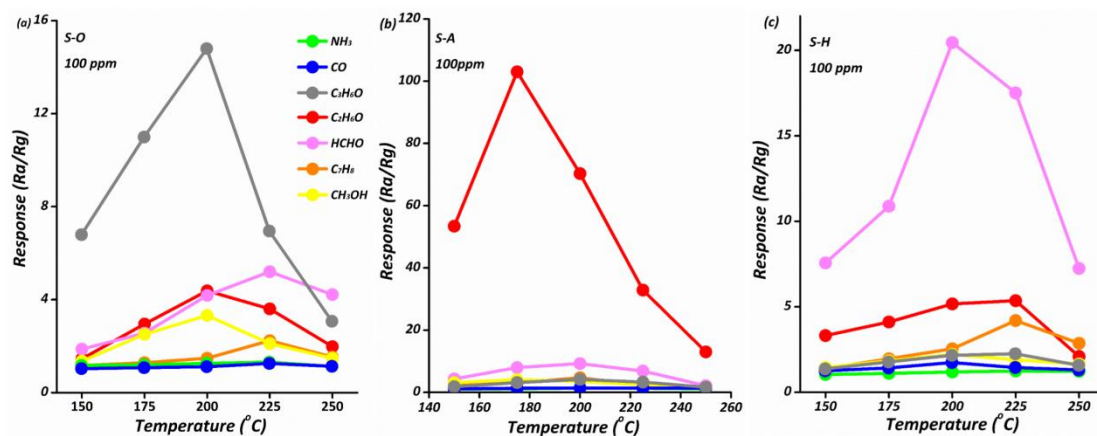


Figure S6 Sensitivity response on exposure to 100 ppm of C₃H₆O, C₂H₆O, CO, NH₃, CH₃OH, C₇H₈, and HCHO gases at different operating temperature for **S-A** NPs (a), **S-H** NPs (b) and **S-O** NPs (c).

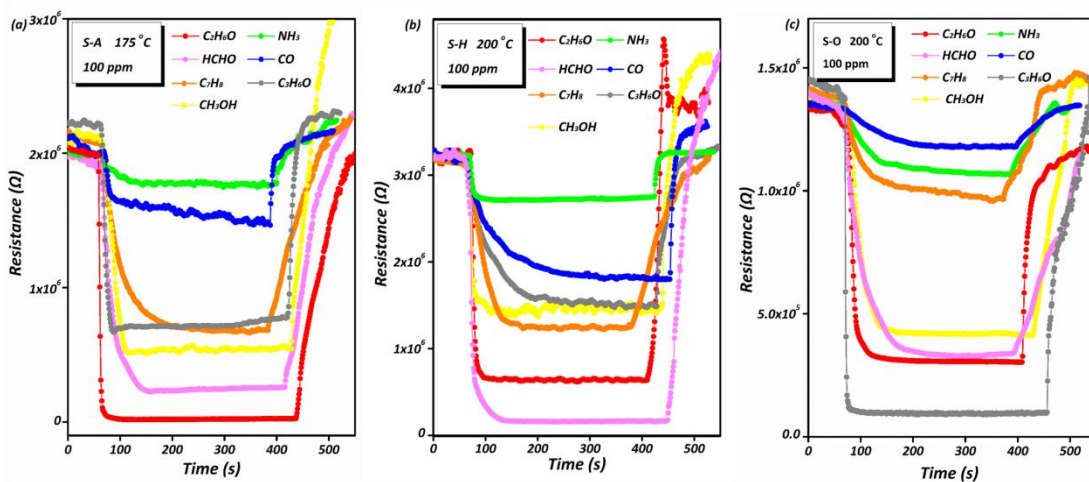


Figure S7. The response curves of sensors based on air, helium and oxygen calcination obtained the **S-A** NPs, **S-H** NPs and **S-O** NPs toward 100 ppm of C₃H₆O, C₂H₆O, CO, NH₃, CH₃OH, C₇H₈, and HCHO at their optimum operating temperature, respectively.

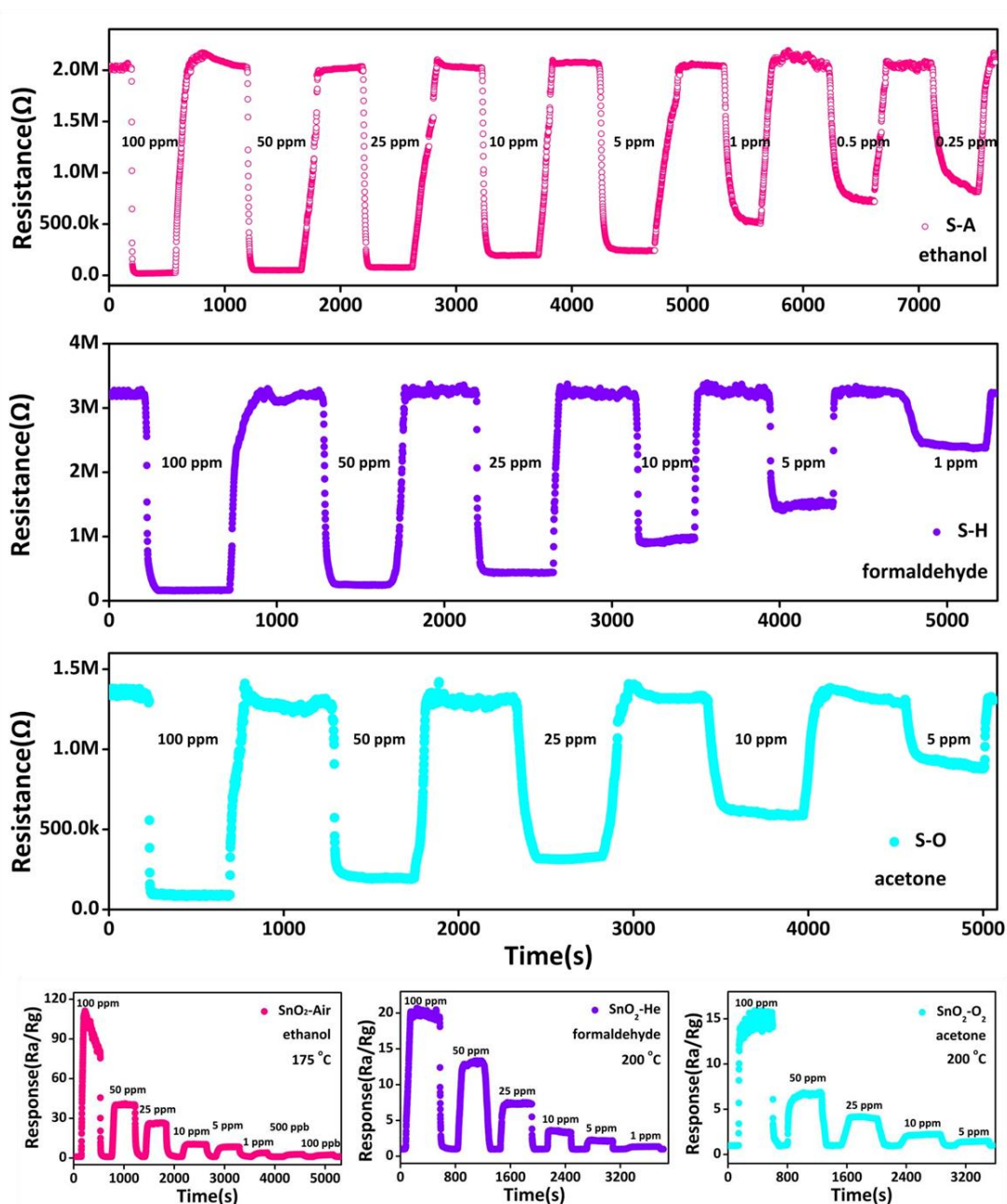


Figure S8. Real-time resistance curves and real-time response curves of the SnO₂ NPs sensors with different defect that the **S-A** response to different concentrations of ethanol at the optimum working temperature of 175 °C, **S-H** response to different concentrations of formaldehyde at the best working temperature of 200 °C, **S-O** upon exposure to different concentrations of acetone (c) at optimum working temperature of 200 °C.

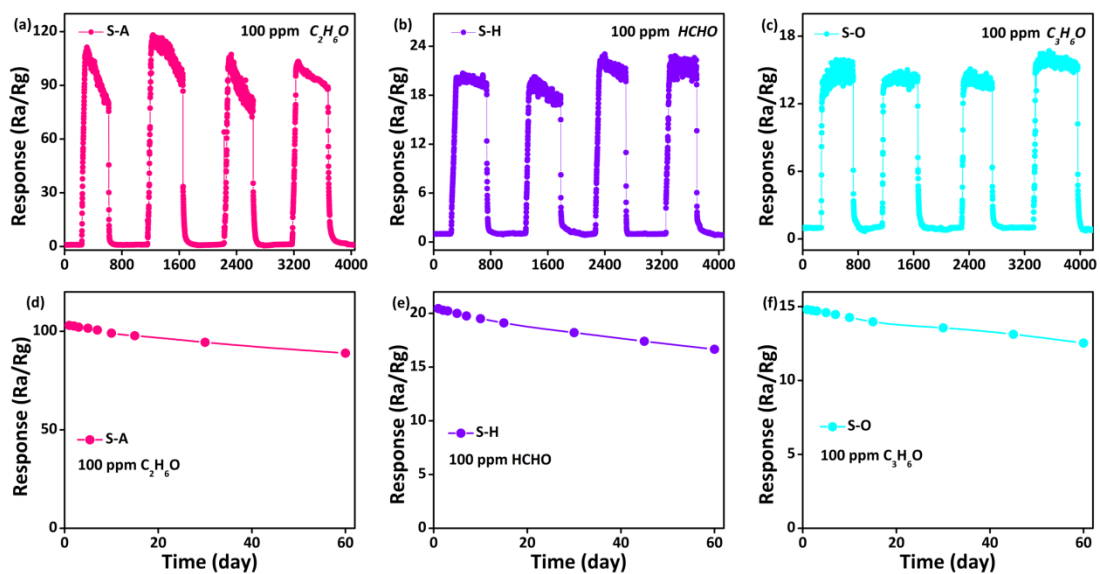


Figure S9. (a, b, c) is the four-cycle repeatability of **S-A**, **S-H**, **S-O**. (d, e, f) long-term stability of the **S-A**, **S-H**, and **S-O** sensor exposed to 100 ppm of ethanol, formaldehyde and acetone gas at respective optimum operating temperatures, respectively.

Table S1. Calculated Positron Lifetime (ps) Values of SnO₂

Defect	bulk	V_{O}^{\bullet}	$V_{Sn}^{\prime\prime\prime}$	$V_{O}^{\bullet\bullet}V_{O}^{\bullet\bullet}$	$V_{Sn}^{\prime\prime\prime}V_{Sn}^{\prime\prime\prime}$	$V_{Sn}^{\prime\prime\prime}V_{O}^{\bullet\bullet}$
Lifetime	154.9	157.1	234.2	160.8	188.2	204.5

Defect	$V_{O}^{\bullet\bullet}V_{O}^{\bullet\bullet}V_{O}^{\bullet\bullet}$	$V_{Sn}^{\prime\prime\prime}V_{Sn}^{\prime\prime\prime}V_{Sn}^{\prime\prime\prime}$	$V_{O}^{\bullet\bullet}V_{Sn}^{\prime\prime\prime}V_{O}^{\bullet\bullet}$	$V_{Sn}^{\prime\prime\prime}V_{O}^{\bullet\bullet}V_{Sn}^{\prime\prime\prime}$
Lifetime	168.6	191	218.6	228.5

References

- (1) Robles, J. M. C.; Ogando, E.; Plazaola, F. Positron lifetime calculation for the elements of the periodic table. *J. Phys.: Condens. Matter* **2007**, *19*, 176222.
- (2) Jiao, X.; Chen, Z.; Li, X.; Sun, Y.; Gao, S.; Yan, W.; Wang, C.; Zhang, Q.; Lin, Y.; Luo, Y.; Xie, Y. Defect-Mediated Electron–Hole Separation in One-Unit-Cell ZnIn₂S₄ Layers for Boosted Solar-Driven CO₂ Reduction. *J. Am. Chem. Soc.* **2017**, *139*, 7586-7594.
- (3) Barbiellini, B.; Puska, M. J.; Korhonen, T.; Harju, A.; Torsti, T.; Nieminen, R. M. Calculation of positron states and annihilation in solids: A density-gradient-correction scheme. *Phys. Rev. B* **1996**, *53*, 16201-16211.